Supporting Information for

A persulfurated benzene molecule exhibits outstanding phosphorescence in rigid environments: from computational study to organic nanocrystals and OLED applications

Giacomo Bergamini,[a] Andrea Fermi,[a,d] Chiara Botta,[c] Umberto Giovanella,[c] Simone Di Motta,[a,b] Fabrizia Negri,[a,b,*] Romain Peresutti,[d,e] Marc Gingras,[d,e*] Paola Ceroni,[a,*]

[a]*Department of Chemistry "G. Ciamician", University of Bologna, 40126 Bologna, Italy*
[b]*INSTM UdR Bologna, 40126 Bologna, Italy*
[c]*ISMAC-CNR,Via Bassini 15, 20133 Milano, Italy*
[d] *Aix-Marseille Universite, CINaM, 163 Ave. de Luminy, 13288 Marseille, France*
[e] *UMR CNRS 7325 Interdisciplinary Center on Nanoscience of Marseille (CINaM), 163 Ave. de Luminy, 13288 Marseille, France*

e-mails of the corresponding authors :
fabrizia.negri@unibo.it ; marc.gingras@univ-amu.fr; paola.ceroni@unibo.it

Synthesis of compounds

Hexakis (4-methylphenylthio) benzene 1:[1,2]

This protocol was based on a previous work. Under an inert atmosphere of argon, hexachlorobenzene (4,51 g.; 16,0 mmol; 1,0 mol-eq), dry potassium carbonate (19,66 g.; 142,2 mmol; 8,9 mol-eq), thiocresol (18,06 g.; 144,4 mmol; 9,0 mol-eq), and dry dimethylformamide (100 mL). The mixture was stirred while heating at 60°C for 40 hours. It turned yellow and the completion of the reaction was monitored by TLC (SiO_2, *n*-hexane/EtOAc 85:15 v/v). While stirring, an aqueous solution of NaOH (2M, 100 mL) was added and a yellow precipitate was filtered. The crude product was triturated with a solution of ethanol/ H_2O (85:15 v/v; 50 mL) while stirring and heating at reflux for 3 hours. After cooling at room temperature, a filtration left a yellow solid, which was rinsed with ethanol (10 mL), and then with diethyl ether (20 mL). After

drying under vacuum, the product was recovered (11,51 g, 90%). For an analytical purity, it was recrystallized from warm toluene to afford some bright yellow crystals The characterization and purity of **1** were in agreement to the literature data.[1,2]

Hexakis (2-isopropylthio) benzene 2

Compound **2** was prepared from a modified protocol of Tiecco et al. [3] Under a nitrogen atmosphere, hexachlorobenzene (1,00 g.; 3,51 mmol; 1,0 mol-eq) was weighed in a flask. 2-Propanethiol (3,9 mL; 3,2 g; 42,1 mmol; 12 mol-eq) was added via a syringe, followed by dry 1,3-dimethyl-2-imidazolidinone (10 mL). The solution was cooled in an ice-bath for several minutes. Via a lateral tube connected to the main flask and containing powdered sodium hydride (1,21 g.; 50,5 mmol, 14 mol-eq), the latter was slowly added within 30 min. while stirring vigorously and by controlling the foam that was being formed. After stirring further for 15 min., the cooling bath was removed and the solution was slowly warmed to ambient temperature and stirred for almost 4 days under nitrogen. After completion of the reaction, an aquous solution of sodium hydroxyde (1M, 200 mL) was poored into the main flask. The crude product was obtained after some extractions with diethyl ether (3 x 100 mL), rinsing with H_2O (2 x 100 mL), drying over anhydrous sodium sulfate, filtration and evaporation of the solvent. It afforded a crude yellow product which was further purified by column chormatography (SiO_2, Et_2O/n-Hexane : 5/95 v/v). Hexakis (2-isopropylthio) benzene was obtained as a yellow solid by keeping the pure fractions (690 mg; 37% yield). The characterization and purity of **2** were in agreement to the literature data.[3,4]

Ground state and lowest triplet excited state geometries of 1 and M2

Four low energy conformers were found for compound **1**, featuring different orientations of the dendrons with respect to the benzene core and two for **M2**. The ground state optimized geometries of the conformers investigated for **1** are shown in Figure S1 and their computed equilibrium energies are also collected in Table S1. The ground state optimized geometries of the conformers investigated for **M2** are shown in Figure S2 and their computed equilibrium energies are collected in Table S1.

To assess the nature of the lowest energy triplet state responsible for the phosphorescence emission of **1,** TD-CAM-B3LYP calculations were carried to identify the lowest triplet states of both **1** and **M2**. These calculations show that the nature of the lowest triplet states is partially benzenoid and partially charge transfer (CT). There are two dominant excitations: one has a benzenoid character since it involves molecular orbitals mainly centred on the central benzene core although they also

extend somewhat to some of the tolyl groups through the sulphur atoms (see Figures S3-S4). The second configuration involves excitation from an occupied orbital localized mainly on the sulphur atoms to an empty benzenoid orbital localized on the benzene core, and therefore it is of CT character. Geometry optimization on a smaller model for compound **2** leads to two triplet structures: the T_2 state whose wavefunction is dominated by the CT character and the T_1 state whose wavefunction is dominated by the benzenoid (BE) character. Because TD-CAM-B3LYP calculations on the larger dendrimers are computationally demanding and difficult to converge, we investigated the triplet potential energy surfaces of compounds **1** and **M2** at UCAM-B3LYP level of theory and explored triplet structures corresponding to the BE and CT excitations.

The validate the quality of the approach chosen (UCAM-B3LYP), we determined the two equilibrium structures of the lowest triplet state of benzene (quinoid and antiquinoid) and in agreement with the known quasi degeneracy of the two structures, we found an energy difference of 0.95 kcal/mol at UCAM-B3LYP level, compared with 0.32 kcal/mol at TD-CAM-B3LYP level, indicating that former level of theory provides acceptable predictions although it is computationally cheaper than the TD-CAM-B3LYP level.

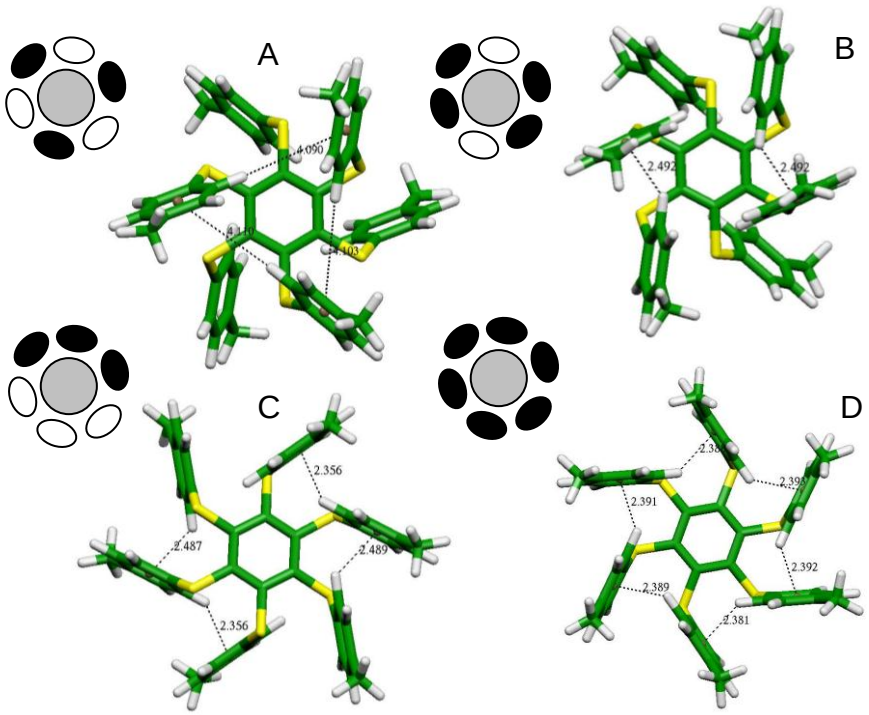

Figure S1. The ground state lowest energy conformers of **1** optimized at B3LYP/3-21G* level of theory. CH-π interactions are evidenced.

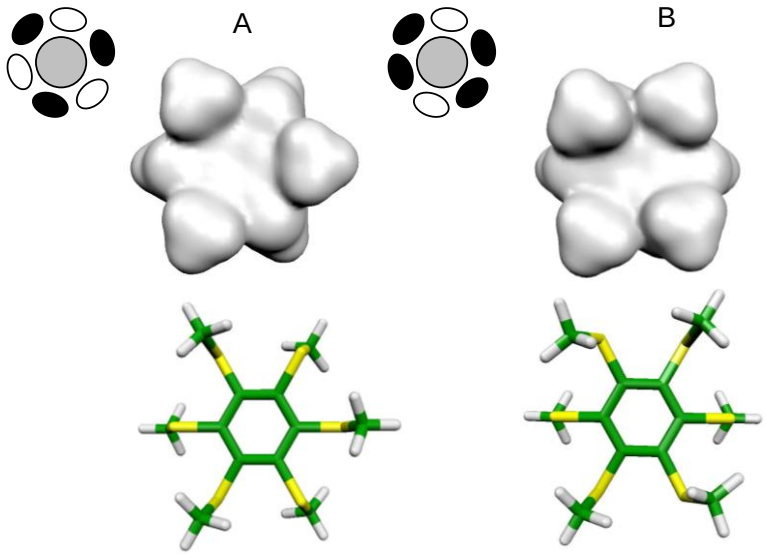

Figure S2. The ground state lowest energy conformers of **M2** optimized at B3LYP/6-31G* level of theory.

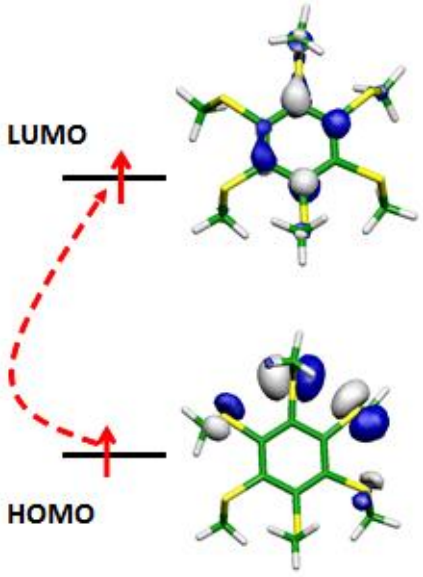

x

Figure S3. The charge transfer (CT) excitation corresponding to the T_2 triplet state structure of **M2**, conformer B, from CAM-B3LYP/6-31G*.

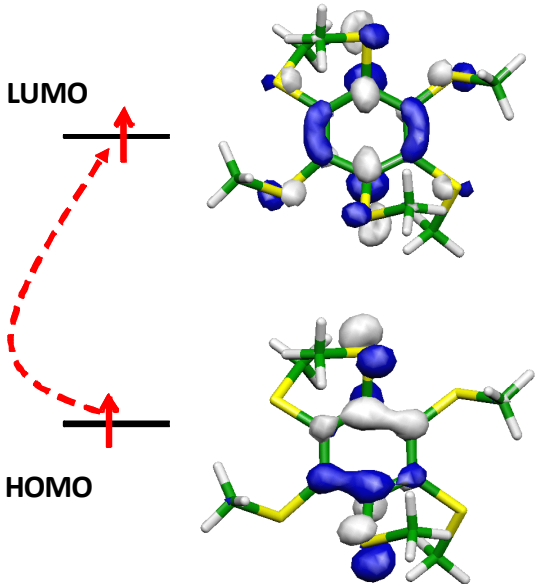

Figure S4. The benzenic (BE) excitation corresponding to the T_1 triplet state structure of **M2**, conformer B, from CAM-B3LYP/6-31G*.

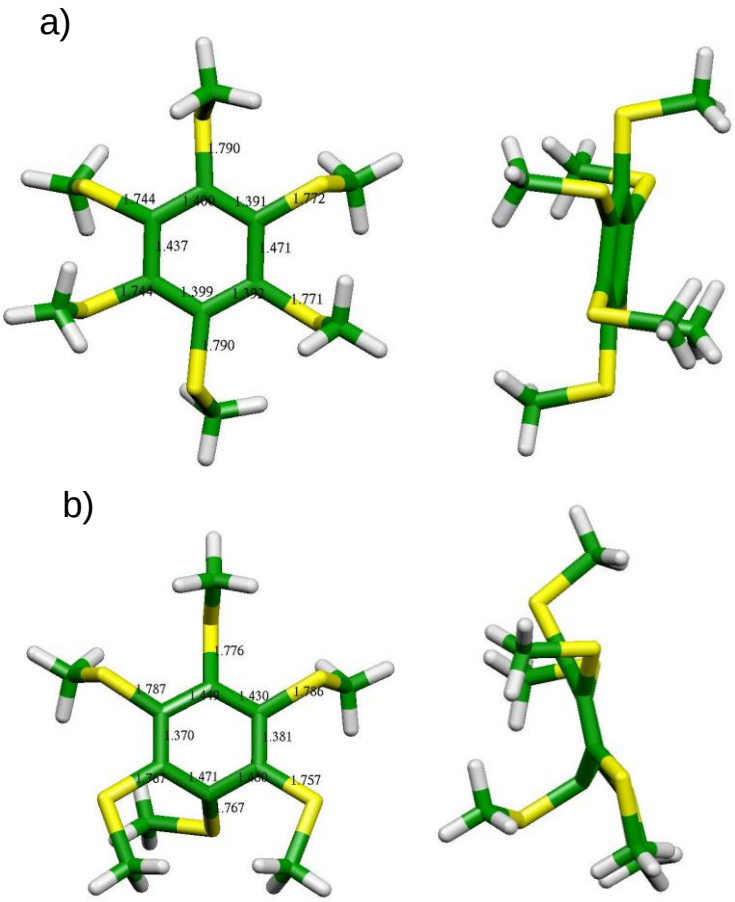

Figure S5. The two UCAM-B3LYP/6-31G* computed triplet state structures of **M2,** conformer A. a) The T_2 state structure with CT character; b) the T_1 state structure with BE character. The S_0-T_1 state inversion occurs at this structure.

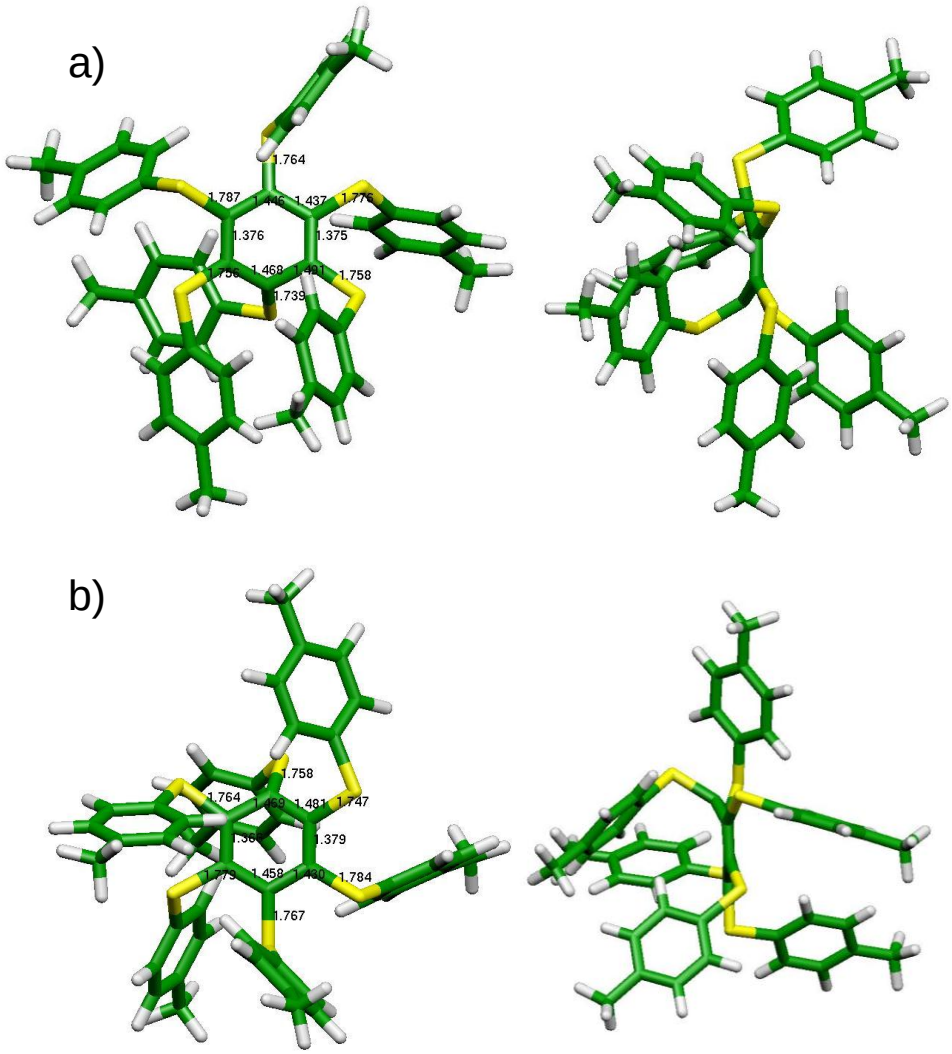

Figure S6. The two UCAM-B3LYP/3-21G* computed triplet state structures of **1,** conformer A. a) The T_1 state structure with BE character. The S_0-T_1 state inversion occurs at this structure.; b) the T_2 state structure with CT character.

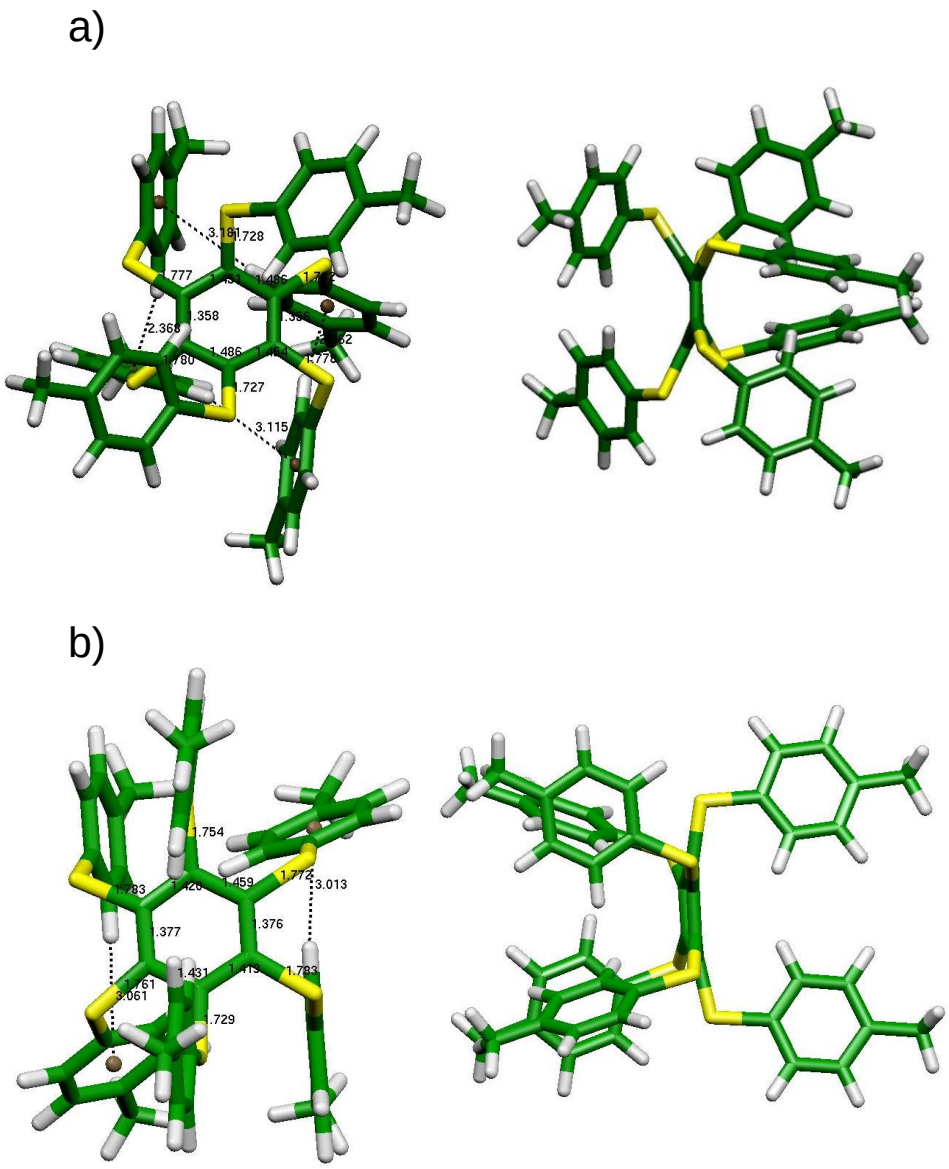

Figure S7. The two UCAM-B3LYP/3-21G* computed triplet state structures of **1,** conformer B. The triplet state is above S_0 at both geometries. a) The T_1 state structure with BE character. ; b) the T_2 state structure with CT character.

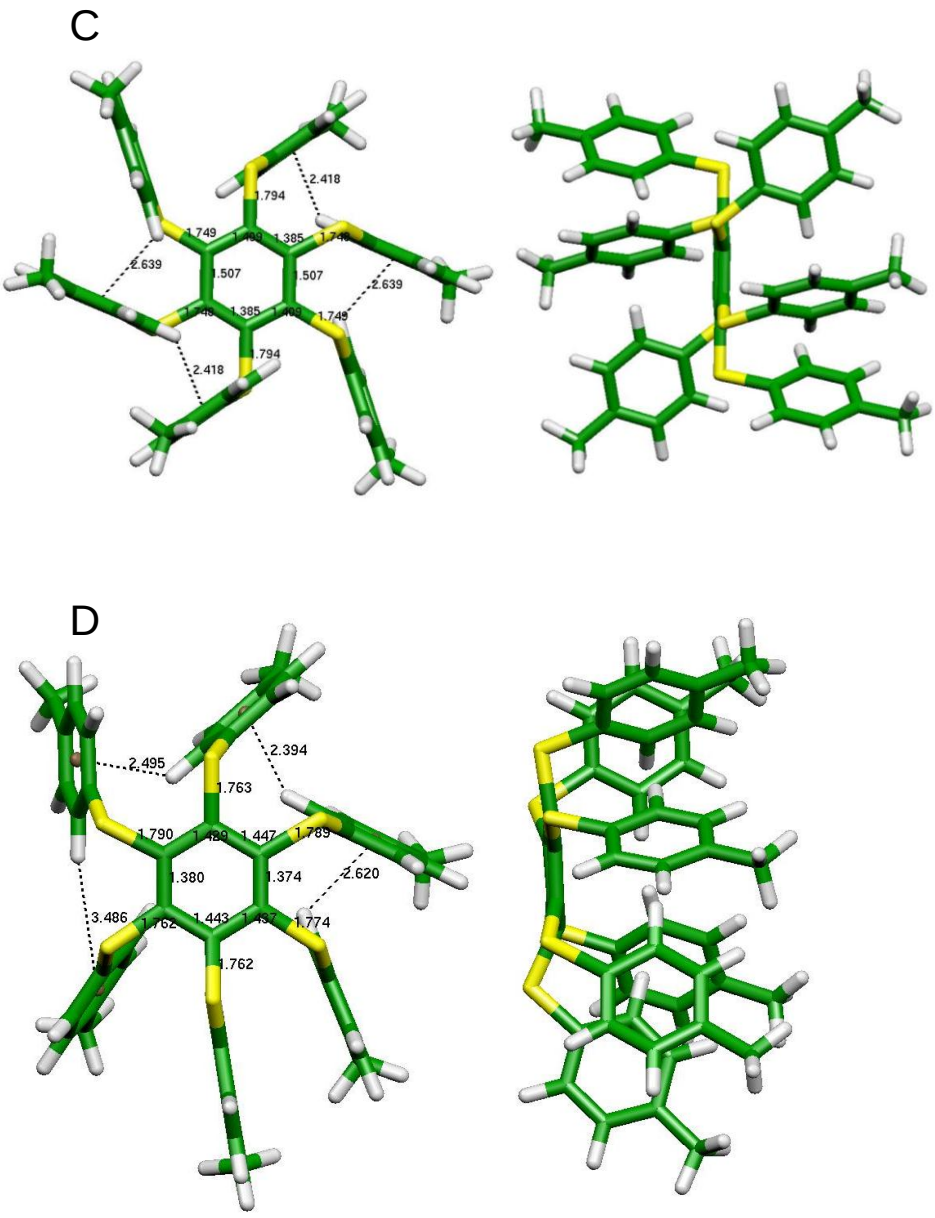

Figure S8. The UCAM-B3LYP/3-21G* computed structure corresponding to the CT triplet state of **1,** conformer C (top) and conformer D (bottom).

Table S1. Computed absolute and relative energies, dipole moment and frontier orbital energies of the different conformers of compounds **1** and **M2** in their ground electronic state

	Absolute energy (a.u.)	Relative energy (kcal/mol)	Dipole moment (Debye)
Compound **M2 CAM-B3LYP/6-31G***			
A	-2856.88765377	0.00	0.00
B	-2856.88352513	+2.59	2.22
Compound **1 CAM-B3LYP/3-21G***			
A	-4221.13270113	+1.79	0.01
B	-4221.13554713	0.00	2.98
C	-4221.13233312	+2.02	0.11
D	-4221.13419959	+0.85	8.76

Table S2. Computed absolute and relative energies of the lowest triplet states, at their optimized UCAM-B3LYP structures, for the different conformers of compounds **1** and **M2**.

Conformer, State, Character	Absolute energy (a.u.)	Relative energy (kcal/mol)	Dipole moment (Debye)	$\Delta E(TD\text{-}CAM\text{-}B3LYP)(S_0\text{-}T_n)$ (eV)
Compound **M2 UCAM-B3LYP/6-31G***				
A, T_2, CT	-2856.77231165	+16.80	4.10	2.49
A, T_1, BE	-2856.79908393	0.00	3.93	-0.86
B, T_2, CT	-2856.77009439	+17.13	4.63	2.54
B, T_1, BE	-2856.79739088	0.00	1.87	-0.42
Compound **1 UCAM-B3LYP/3-21G***				
A, T_1, BE	-4221.03868395	+1.55	4.60	-0.51
A, T_2, CT	-4221.03114400	+6.29	1.58	+0.31
B, T_1, BE	-4221.04115993	0.00	2.73	+0.86
B, T_2, CT	-4221.02596234	+9.54	6.10	+2.41
C, T_2, CT[a]	-4221.02686295	+8.97	0.00	+2.09
D, T_2, CT[a]	-4221.02170417	+12.21	10.79	+2.25

[a] For conformers C and D only the CT triplet state structure could be determined.

Table S3. Validation of the computational approach: Computed absolute and relative energies of the quinoid and antiquinoid structures of the lowest triplet electronic state of benzene.

	Absolute energy (a.u.)	Relative energy (kcal/mol)	$\Delta E(TD\text{-}CAM)(S_0\text{-}T_1)$ (eV)
Triplet Benzene **UCAM-B3LYP/3-21G**			
quinoid	-230.682293691	+0.95	2.71
antiquinoid	-230.683814369	0.00	2.77
Triplet Benzene **TD-CAM-B3LYP/3-21G**			
quinoid	-230.705158116	0.00	2.72
antiquin	-230.704654588	+0.32	2.76

Dynamic Light Scattering measurements

Measurements have been carried out taking into account the average of 4 consecutive experiments consisting of 4 series of 15 runs each.

			Size (d.nm):	% Intensity	Width (d.nm):
Z-Average (d.nm):	102,1	Peak 1:	103,7	100,0	18,20
PdI:	0,069	Peak 2:	0,000	0,0	0,000
Intercept:	0,961	Peak 3:	0,000	0,0	0,000
Result quality :	Good				

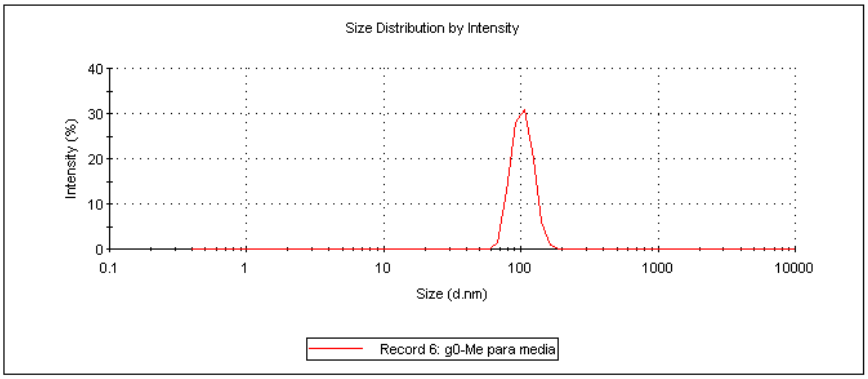

Figure S9. Size distribution versus recorded intensities (%) on an aqueous dispersion of **1**.

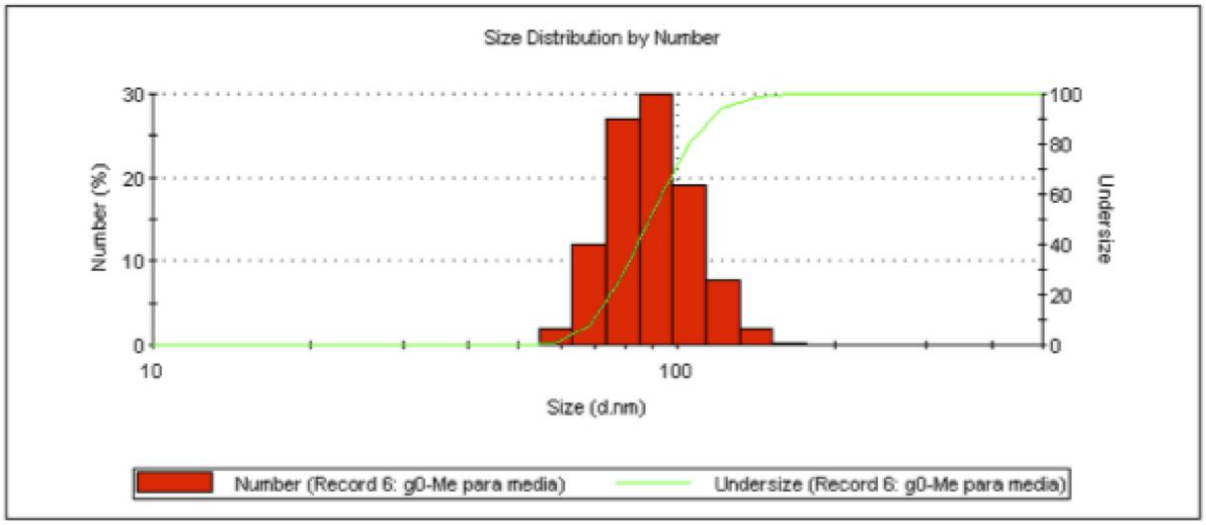

Figure S10. Distribution histogram versus calculated number of particles (%) from an aqueous dispersion of **1**. The green line refers to the cumulative frequency distribution of the size of the nanoparticles.

Photophysical properties of aqueous NPs of 1

The suspension used to carry out DLS analysis has been characterized by UV-vis absorption and phosphorescence emission. Details: UV/Vis absorption spectra were recorded with a Perkin Elmer l40 spectrophotometer; fluorescence spectra were obtained with a Perkin Elmer LS-50 spectrofluorimeter, equipped with a Hamamatsu R928 phototube. The estimated experimental errors are: 2 nm on the band maximum, 5% on the molar absorption coefficient.

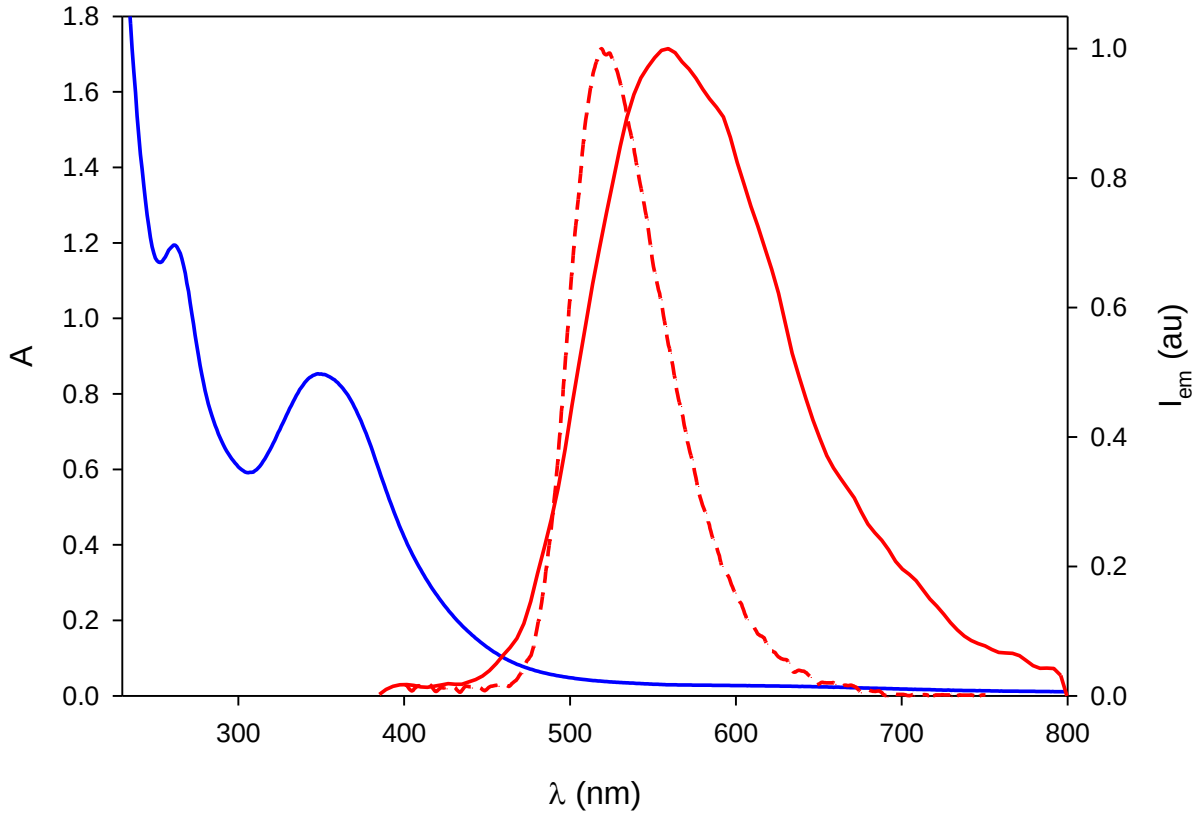

Figure S11. Absorption spectrum (blue line) and phosphorescence spectrum (red line, λ_{ex}=300 nm, delay time=0.05 ms, gate time=1 ms) of dispersion of aqueous nanoparticles of **1**. The emission of **1** as a powder is reported for comparison (red dashed line).

Electroluminescence

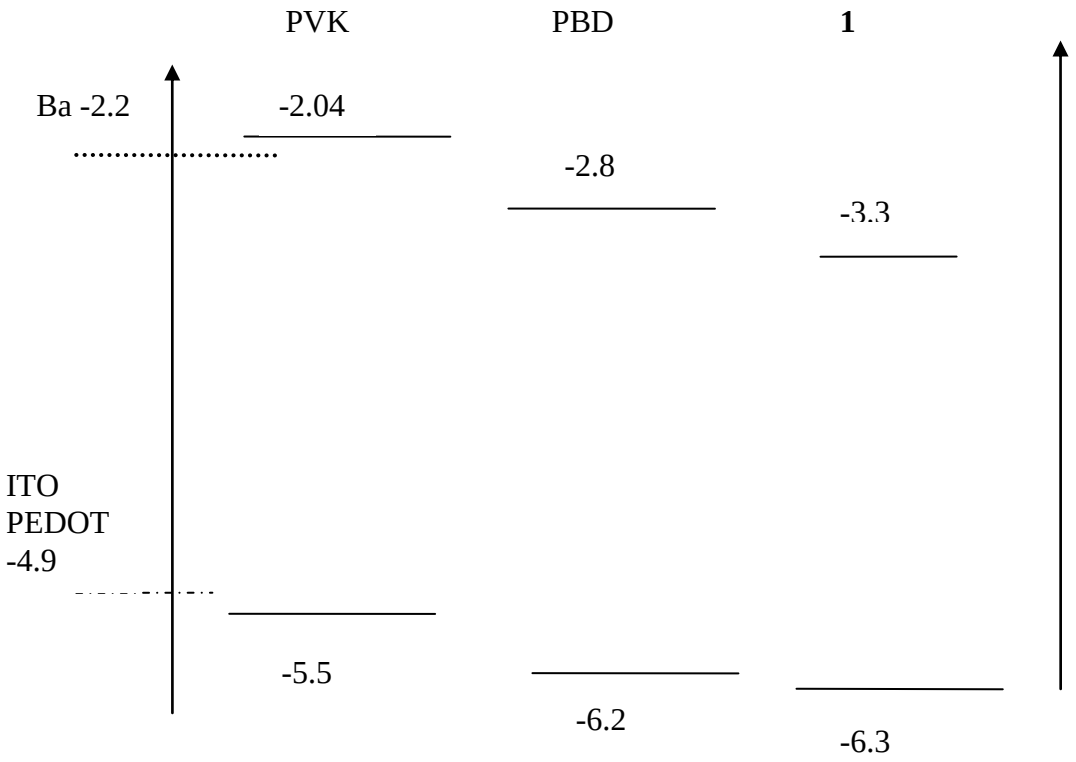

Figure S12. Scheme of the HOMO and LUMO energy levels of the materials used in the LED and of the work functions of the electrodes (left side). Values are in eV with respect to vacuum. For compound **1**, the LUMO level has been estimated from the reduction potential (-1.42 V vs SCE).

[1] J. H. R. Tucker, M. Gingras, H. Brand, J.-M. Lehn, *J. Chem. Soc. Perkin Trans. II*, 1997, 1303-1307.

[2] Previous syntheses of **1**: (a) M. Arisawa, T. Suzuki, T. Ishikawa, M. Yamaguchi, *J. Am Chem. Soc.*, 2008, **130**, 12214-12215. (b) Y. Suenaga, K. Kitamura, T. Kuroda,-Sowa, M. Maekawa, M. Munakata, *Inorg. Chim. Acta*, 2002, **328**, 105-110. (c) A. D. U. Hardy, D. D. MacNicol, D. R. Wilson, *J. Chem. Soc. Perkin Trans 2*, 1979, 1011-1019. (d) B. F. Malichenko, L.P. Robota, *Zh. Org. Khim*., 1975, **11**, 778-782.

[3] L. Testaferri, M. Tingoli, M. Tiecco, *J. Org. Chem.*, 1980, **45**, 4376-4380.

[4] (a) A. Alberti, G. F. Pedulli, M. Tiecco, L. Testaferri, M. Tingoli, *J. Chem. Soc. Perkin Trans 2*, 1984, 975-979. (b) L. Testaferri, M. Tiecco, M. Tingoli, D. Chianelli, M. Montanucci, *Synthesis*, 1983, 751-755.